© 2013

# Proposed Model for Biomineralization of Novel Nanohydroxyapatite/Vertically Aligned Multiwalled Carbon Nanotube Scaffolds

*Tayra Rodrigues Brazil*[a], *Marcele Florêncio das Neves*[a], *Inacio Regiani*[b],

*Fernanda Roberta Marciano*[a], *Anderson Oliveira Lobo*[a]*

[a]*Laboratory of Biomedical Nanotechnology, Universidade do Vale do Paraíba – Univap,*
*Av. Shishima Hifumi, 2911, CEP 12224-000, São José dos Campos, SP, Brazil*
[b]*Instituto Tecnológico de Aeronautica – ITA, Praça Marechal Eduardo Gomes, 50, CEP 12228-900,*
*São José dos Campos, SP, Brazil*

For the first time, the growth mechanism of biominerals formed on plate-like nanohydroxyapatite (nHAp) electrodeposited on superhydrophilic vertically aligned multi-walled carbon nanotubes (VAMWCNT-$O_2$) is presented and a model for the specific growth preference is discussed. VAMWCNT-$O_2$ films were obtained by microwave-assisted chemical vapor deposition method and funcionalized by oxygen plasma. nHAp/VAMWCNT-$O_2$ nanocomposites were fabricated with a direct electrodeposition of the thin nHAp films onto the VAMWCNT-$O_2$ films. The biomineralized "scaffolds" were obtained by soaking nHAp/VAMWCNT-$O_2$ in simulated body fluid for 7, 14 and 21 days. Results show that the carboxyl functional groups directly attached onto VAMWCNT tips after oxygen plasma treatment were essential for the acceleration of the OH- formation and the deposition of plate-like nHAp crystals.

**Keywords:** *biomineralization, carbon nanotubes, vertically aligned, superhydrophilic, nanohydroxyapatite, SBF, characterization techniques*

## 1. Introduction

Multi-walled carbon nanotubes (MWCNT) are stable structures that can be associated to other molecules to be used in many applications. Due to its physical-chemical properties, these nanostructures can biomimic the nanocharacteristics of living tissues. This mimetic process can favor cell adhesion and proliferation over its surface, and making MWCNT a promising alternative to bone regeneration[1-4]. Its properties and biocompatibility are improved when MWCNT becomes vertically aligned (VAMWCNT) and superhydrophilicity (VAMWCNT-$O_2$)[5].

VAMWCNTs-$O_2$ are of particular interest for regenerative medicine due to their biocompatibility. Coating VAMWCNTs-$O_2$ with nanohydroxyapatite (nHAp) through electrodeposition process permits extensive cell adhesion, spreading, and growth. nHAp can establish chemical bonds between the material and the bone tissue due to its similarity to bone mineralized matrix[6]. nHAp/VAMWCNT-$O_2$ has been shown to support the growth of osteoblast cells by stimulating ECM production in bone tissue formation and growth of nHAp crystals[7].

The mechanism of osteointegration can be divided in three phases. First, osteoinduction based on cells adhesion. The capacity of the cells to adhere to the implant's surface depends on this matrix. Only after adhered, cells can start the second stage, where their attachment and spreading processes take place. Finally, migration and differentiation over implant's surface that results in a mineralized matrix. The remodelation creates the bone-implant interface that consists on the formation of a new bone tissue. The implant's characteristics and patient's metabolism interfere on bone regeneration process[8,9].

In addition to the application of nHAp/VAMWCNT-$O_2$ as "scaffolds", the process of biomineralization by incubating the samples in SBF (5×) (ion concentrations similar to human extracellular fluid) assists the development of biological apatites on the surface of nHAp/VAMWCNT-$O_2$[10].

The present study showed, for the first time, the results of biomimetized mineralization on nHAp deposited over functionalized VAMWCNT-$O_2$ using SBF (5×) a pH 6.10 for 7, 14 and 21 days, seeking for different crystals morphologies and designs.

## 2. Material and Method

### 2.1. *Synthesis of vertically aligned multi-walled carbon nanotubes (VAMWCNT)*

The VAMWCNT were produced as thin films using a microwave plasma chamber equipped with a 2.45 GHz microwave generator (MWCVD). The substrates were 10 mm titanium (Ti) squares covered by a thin Fe layer (10 nm) deposited by an e-beam evaporator. The Fe layers

were pre-treated to promote nanocluster formation, which forms the catalyst for VAMWCNT films growth. The pre-treatment was carried out for 5 minutes in plasma atmosphere of $N_2/H_2$ (10/90 sccm) with a substrate temperature of around 760 °C. After pre-treatment, $CH_4$ (14 sccm) was inserted into the chamber at a substrate temperature of 800 °C for 2 minutes. The reactor was kept at a pressure of 30 Torr during the entire process[6].

## 2.2. *VAMWCNT functionalized by polar groups*

Functionalization of the VAMWCNT tips by the incorporation of oxygen-containing groups was performed in a pulsed-direct current plasma reactor with an oxygen flow rate of 1 sccm, at a pressure of 85 mTorr, –700 V, and with a frequency of 20 kHz. The total time of the plasma etching was 120 seconds. Detailed descriptions of the superhydrophilic properties to produced VAMWCNT-$O_2$ are given elsewhere[6].

## 2.3. *nHAp/VAMWCNT-$O_2$ nanocomposites fabrication*

The electrodeposition of the nHAp crystals on the VAMWCNT-$O_2$ films were performed using 0.042 mol $L^{-1}$ $Ca(NO_3)_2.4H_2O$ + 0.025 mol $L^{-1}$ $(NH_4)_2HPO_4$ electrolytes (pH 4.7). The electrochemical measurements were carried out using a three-electrode cell coupled to an Autolab PGSTAT128N instrument. VAMWCNT-$O_2$ films were used as the working electrode and the geometric area in contact with electrolytic solution was 0.27 $cm^2$. A platinum coil wire served as the auxiliary electrode and an Ag/AgCl electrode was used as the reference electrode. The nHAp films were produced by applying a constant potential of –2.0 V for 30 minutes while the solution temperature was maintained at 70 °C[6].

## 2.4. *Biomineralization of nHAp/VAMWCNT-$O_2$ nanocomposites*

The SBF (5×) solution was prepared by dissolving ions in distilled water at a stir plate. The SBF (5×) compositions used were proposed by Barrere et al.[11,12] (Table 1), whose components concentration are five times higher than the original solution proposed by Kokubo[13] and solution pH 6.10 was adjusted by adding HCl using a pH meter (Metrohm).

nHAp/VAMWCNT-$O_2$ nanocomposites were immersed into a corning tube with 15 mL of each SBF (5×) pH solution adjusted to 6.10 for 7, 14 and 21 days, placed in refrigerated bench top incubator (Cientec CT-712-R), shaken at 75 rpm at a temperature around 36.5 °C. After the immersion period the samples were removed from the SBF (5×) solution, washed with hot distilled water and oven dried for 24 hours

at 50 °C. The objective of this methodology was obtained different apatites formations on nHAp/VAMWCNT-$O_2$ nanocomposites.

## 2.5. *Characterization of nHAp/VAMWCNT-$O_2$ nanocomposites*

To carry out the morphological analysis of all types of samples analyzed in this study, a scanning electron microscope was used (SEM, model: JEOL-JSM 5610 VPI). Images were recorded at magnification of 1000-100,000×.

Semi-quantitative elemental analyses of calcium and phosphorus were carried out by micro energy-dispersive X-ray fluorescence (μ-EDXRF) (1300, Shimadzu, Kyoto, Japan), equipped with a rhodium X-ray tube and a Si (Li) detector cooled by liquid nitrogen ($N_2$). The energy range of scans was from 0.0 to 40.0 eV. The voltage in the tube was set at 15 kV.

The structural analysis of apatites formed on the nHAp/VAMWCNT-$O_2$ surface were performed at room temperature by X-ray diffractometry (XRD) with CuK-α radiation (α = 0.154056 nm) from 10 to 70° in 2-theta with the condition voltage of 40 kV, current of 30 mA, step size of 0.02°, and a counting time of 2 seconds per step (Model: X`Pert MRD, Philips).

## 3. Results and Discussion

SEM (Figure 1a) and TEM (Figure 1b) show examination structure of the VAMWCNT-$O_2$ revealed no morphologic change in both samples. Samples functionalized with oxygen did not suffer any corrosion or decreasing of thickness after the plasma treatment. Figure 1a shows that oxygen plasma do not influenced in vertically aligned of the MWCNTs. After the treatment (Figure 1b) it was observed that there were no changes on VAMWCNT-$O_2$ structure, no significant thickness reduction or abrupt corrosive processes, since they

**Table 1.** SBF (5×) components and concentration.

| Reagent | Quantity (mM) |
|---|---|
| NaCl | 733.5 |
| $MgCl_2.6H_2O$ | 7.5 |
| $CaCl_2.2H_2O$ | 12.5 |
| $Na_2HPO_4.2H_2O$ | 5.0 |
| $NaHCO_3$ | 21.0 |



(a)  (b)

(c)  (d)
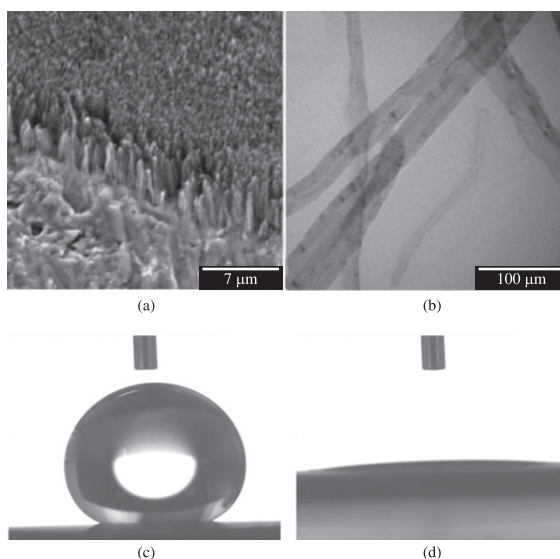
**Figure 1.** SEM (a) and TEM (b) showing the morphology and structure of VAMWCNT-$O_2$; Optical microscopy images of the contact angle between deionized water and VAMWCNT before (c) and after (d) the oxygen plasma treatment (magnification 9200).

2013; 16(3)

Proposed Model for Biomineralization of Novel Nanohydroxyapatite/Vertically
Aligned Multiwalled Carbon Nanotube Scaffolds

663

retain the same dimensions of VAMWCNT-O$_2$ (Figure 1a) and also not suffer from structural changes.

The potential biomedical application of the VAMWCNT is limited due to its hydrophobicity[14]. Several methods are used to control wettability of VAMWCNT, including forming oxygen-containing functional groups on its surfaces by oxidative treatment[15] or acid treatment[16]. The wettability in polar liquids, such as water, improved significantly in this way, leading to more reactive VAMWCNT surfaces[17]. The oxygen plasma etching is the most efficient way to introduce polar groups (COH, OH, C=O, COOH) and roughness to VAMWCNT in order to obtain superhydrophilic behavior[18].

Figures 1c and 1d show the efficiency of the oxygen plasma treatment on converting VAMWCNT surfaces from superhydrophobic to superhydrophilic behavior, comparing contact angle between deionized water on VAMWCNT before (1c) and after (1d) the oxygen plasma treatment. The superhydrophilicity of the VAMWCNT films obtained after the oxygen plasma treatment (VAMWCNT-O$_2$) was a requirement to obtain nHAp/VAMWCNT-O$_2$ nanocomposites by the electrodeposition method to achieve excellent bioactivity.

The –COOH groups formed on superhydrophilic VAMWCNT films after the oxygen plasma treatment (Figure 1b) constructed ordered ''recognized sites'' with high polarity and charged density, which could draw the direct electrodeposition of the nHAp on them.

Liao et al.[19] suggested that dispersed VAMWCNTs provide abundant sites for nucleation of nHAp soaked in phosphate solution. They showed that the bamboo-like structure can be attributed to nucleation sites for nHAp formation. The electrodeposition of nHAp (data shown in Figure 3a) indicates that the growth only occurs on the top surface of the VAMWCNT-O$_2$. This top surface is heavily attacked by oxygen plasma, which is responsible for the grafting of the oxygen groups onto VAMWCNT-O$_2$ and a further roughening of the VAMWCNT-O$_2$ surfaces. Clearly, the rapid and direct electrodeposition of plate-like nHAp crystals on VAMWCNT-O$_2$ films is highly influenced by the COOH groups and VAMWCNT-O$_2$ rough nanotopology surface[18].

The mechanism for nHAp crystal formation on VAMWCNT-O$_2$ films was already proposed and discussed in literature[18]. The schematic reaction ilustration of plate-like nHAp crystals formation and dissolution during direct electrodeposition on VAMWCNT-O$_2$ to form nHAp/VAMWCNT-O$_2$ composite is shown in Figure 2[18].
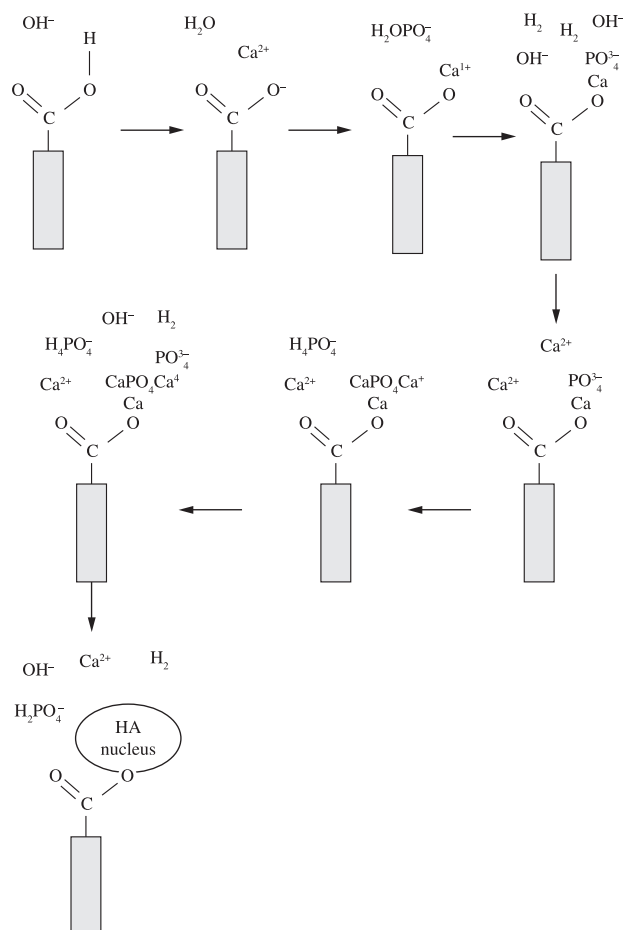


**Figure 2.** Schematic illustration of plate-like nHAp crystals formation and dissolution during direct electrodeposition on VAMWCNT-O$_2$s surfaces based on Lobo et al model[18].

Figure 3 shows SEM micrography of nHAp/VAMWCNT-O$_2$ surfaces before (Figure 3a) and after biomineralization process (Figure 3b-d). nHAp crystalls grown over VAMWCNT-O$_2$ by electrodeposition are shown in Figure 3a. All crystals are plate-like and have thickness about few dozens of nanometers (data not shown).

All samples showed uniform plate-like nHAp crystal with distinct orientations over VAMWCNT-O$_2$ film, identifying the electrodeposition processes homogeneity (Figure 3a). Biominiralization was successfully induced over nHAp/VAMWCNT-O$_2$ by SBF (5×) as can be seen in Figure 3b-d.

After electrodeposition process, nHAp/VAMWCNT-O$_2$ surface is negatively charged and selectively combined with Ca ions positively charged, forming polycrystalline nanoapaties[20]. As Ca ions accumulate on the biomaterial surface, it becomes positively charged and these ions combine with phosphate ions negatively charged, forming calcium phosphates[21]. The calcium phosphate apatite spontaneously turns, simulating the many phases of the chemical calcium phosphate present in biological tissues such as bone, which justifies its use as nanobiomaterial[22].

In the first 7 days there are only plate-like nanocrystals of nHAp, with no precipitation. However, it is possible to see that these crystals had started to change their morphology to a cluster shape (Figure 3b). After 14 days, it is possible to note a growth in the size and numbers of nHAp clusters forming a dense layer, as well as a second layer of nHAp over the plate-like nanocrystals (Figure 3c). In Figure 3d, it is possible to note that this second layer of nHAp precipitated from SBF (5×) is denser but not uniform or homogeneous due to the different sizes and location of nHAp crystals clusters and full of valleys, showing a good biomimetism. It is possible to conclude that these morphologic changes in layer and the presence of polycrystaline apatites are due to immersion time: as longer as the samples get immersed in SBF (5×), as thicker the layer will become due to Ca ions preciptation and nucleation, followed by P ions, consequently.

Some influential factors are considered in ions of Ca and P dissolution, being a key for microstructural features, like grain size and pore distribution. It is known that a high porosity and small grain size increases the dissolution rate. Nanosized pores can also act as sites for early nucleation and growth of apatite crystals[23].

Figure 4 shows μEDX mapping made on biomineralized samples. The first column (Figure 4a, d, g) shows the delimited area for the analysis, the second column (Figure 4b, e, h) the mapping related to Ca distribution and the third column (Figure 4c, f, i) the mapping related to P.



(a)  (b)  (c)  (d)
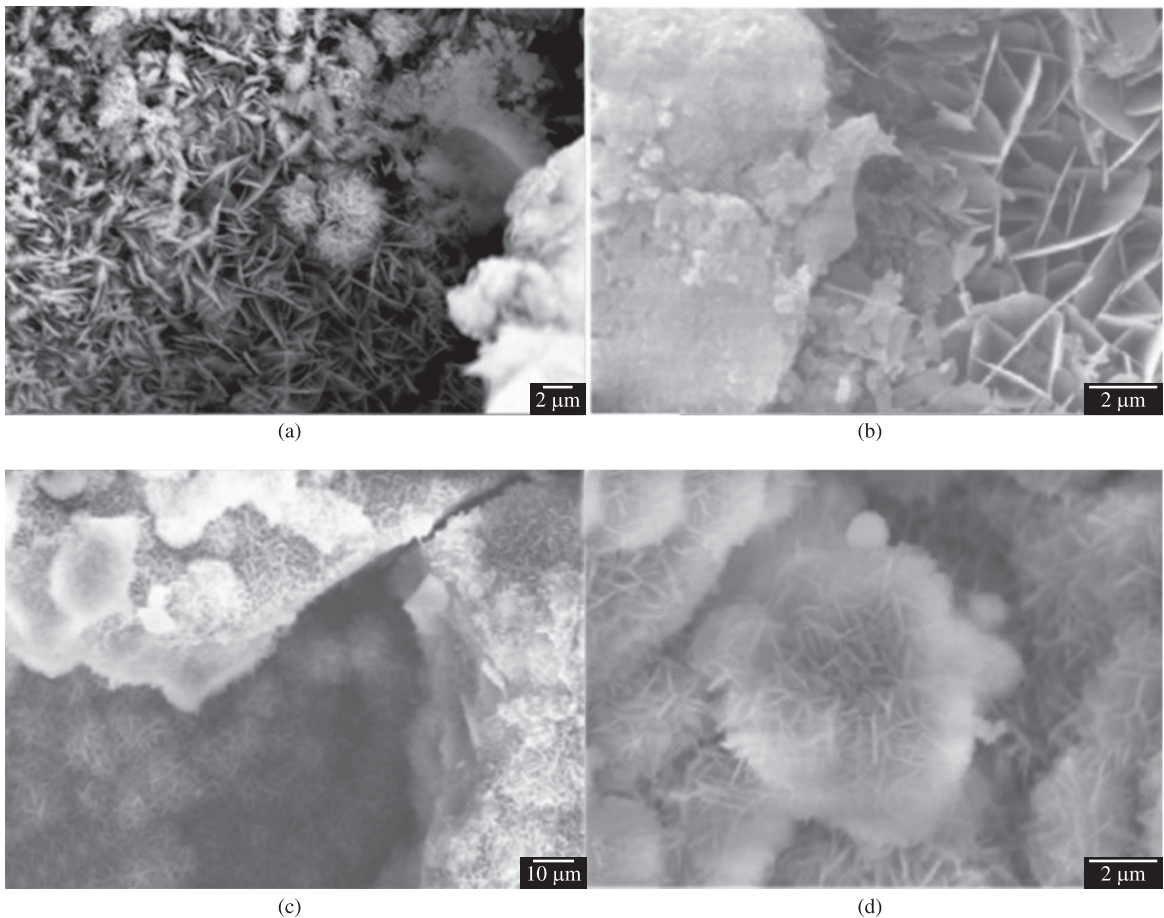
**Figure 3.** SEM images of nHAp/VAMWCNT-O$_2$ nanocomposites before (a) and after SBF (5×) immersion for 7 (b), 14 (c) and 21 (d) days.

2013; 16(3)

Proposed Model for Biomineralization of Novel Nanohydroxyapatite/Vertically
Aligned Multiwalled Carbon Nanotube Scaffolds

665
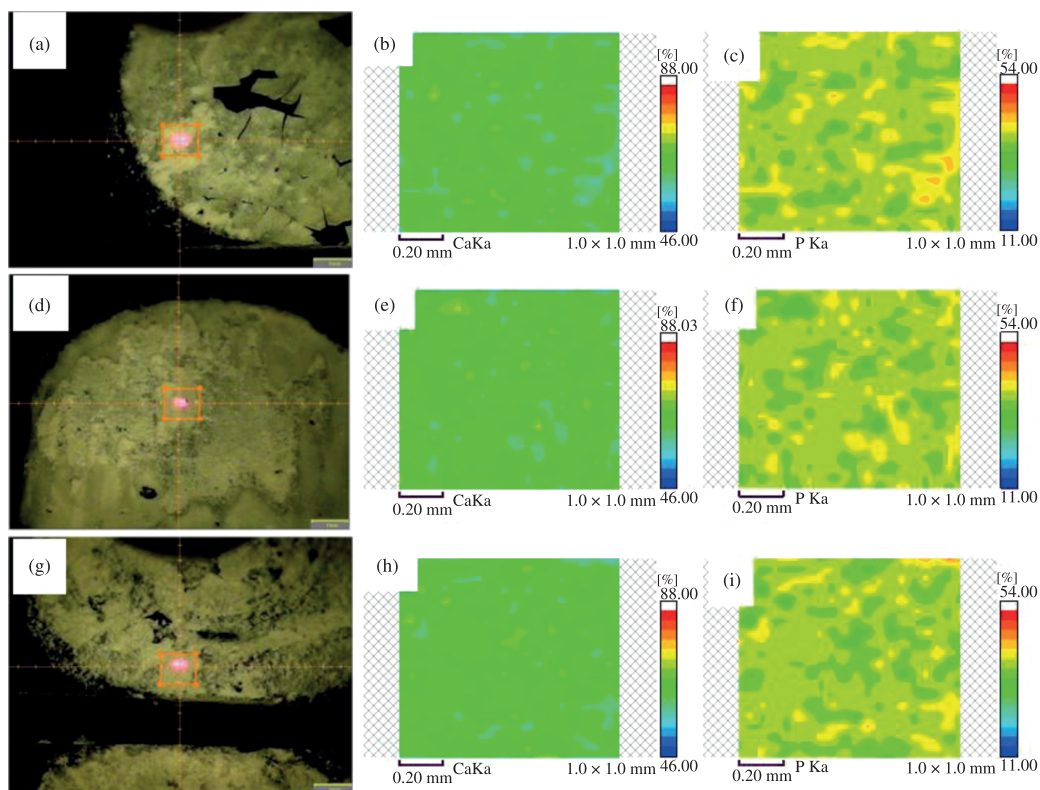


**Figure 4.** μEDX mapping of Ca and P for 7days (a, b, c), 14 days (d, e, f) and 21 days (g, h, i).

The lines are related to the SBF (5×) soaking period, first for 7 days (Figure 4a, b, c), second for 14 days (Figure 4d, e, f) and third for 21 days (Figure 4g, h, i).

It is possible to note that Ca is more homogeneously and well distributed over the surface (Figure 4b, e, h) than P that shows heterogeneities points with higher concentration (Figure 4c, f, i). Despite Figure 4 do not show any significant differences between the biomineralized samples, the Ca/P ratio from the semi-quantitative analysis provided by the μEDX (Table 2) shows a discrete increasing proportional to the SBF (5×) immersion time.

The μEDX analyses show a Ca/P ratio increasing from 1.743 to 1.776 in biomineralized samples, near to bone nHAp Ca/P ratio of 1.71[24], proving the biomineralized nHAp/VAMWCNT-O$_2$ bioactivity and Ca ions precipitation earlier than P ions.

Calcium is one of the most present elements in SBF (5×) and bioactive materials, whose participation is very effective in the process of dissolution/precipitation. The release of this ion is responsible for the biologically active layer formation and works as stimulus for bone growth[25].

X-ray diffractogram (Figure 5) shows typical nHAp and Ti peaks at: 25.9° (002); 32.2 (112) e 32.9 (300) reflections.

Comparing nHAp/VAMWCNT-O$_2$ nanocomposites before and after SBF (5×) immersion, the reflections at 25.9° attributed to the presence of nHAp crystals, are narrower and more intense according to SBF (5×) incubation time. It can be noted that with at 14 and 21 days of Ti peaks are no longer so intense. This finding refers to the increase of nHAp layer

**Table 2.** Weight percentages of Ca and P in the biomineralized layer.

| Sample | Calcium (Ca) | Phosphor (P) | Ca/P ratio |
|---|---|---|---|
| 7 days | 63.55 | 36.450 | 1.743 |
| 14 days | 63.94 | 36.062 | 1.773 |
| 21 days | 63.98 | 36.015 | 1.776 |

[#]Ca/P of as grown nHAp is 1.145.
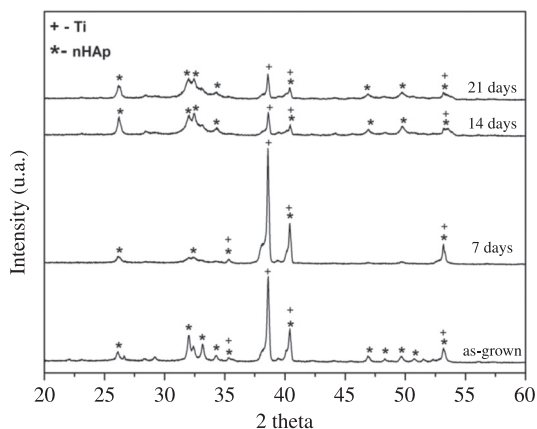


**Figure 5.** X-Ray Diffraction of nHAp/VAMWCNT-O$_2$ nanocomposites.

thickness proportional to the incubation time in SBF (5×) solution (Figure 3c, d). It is proposed that the larger the time in soaking SBF (5×), the greater Ca precipitation (Table 2).

Considering the results of µEDX mapping, the broadening of nHAp crystals peaks in the XRD and the Ca/P, it is possible to affirm that the biomineralization produce a layer of nHAp crystals in a matrix of amorphous calcium phosphate.

## 4. Conclusion

The results presented are innovative since this biomineralization process hadn't been performed on nHAp/VAMWCNT-O$_2$ nanocomposites yet. Different morphologic nanocrystals were obtained according to the SBF (5×) immersion time. Best results were obtained when nHAp/VAMWCNT-O$_2$ nanocomposites were immersed in SBF (5×) for 21 days, which certainly facilitates the incorporation of Ca ions, accelerating precipitation of P ions. It can be stated that the denser layer composed for plate-like crystal and clusters with pores and valleys on nHAp/VAMWCNT-O$_2$ nanocomposites surface have characteristics and properties that may collaborate with regenerative processes to formation of bone tissue because its similarities with natural cortical bone what can provide a adhesion and proliferation of humans osteoblasts cells.

## References

1. Lobo AO, Corat MAF, Antunes EF, Ramos SC, Pacheco-Soares C and Corat EJ. Cytocompatibility studies of vertically-aligned multi-walled carbon nanotubes: Raw material and functionalized by oxygen plasma. *Materials Science and Engineering:* C. 2010; 32(4):648-652. http://dx.doi.org/10.1016/j.msec.2010.08.010

2. Webster TJ, Waid MC, McKenzie JL, Price RL and Ejiofor JU. Nano-biotechnology: carbon nanofibres as improved neural and orthopaedic implants. *Nanotechnology*. 2004; 15(1):48-54. http://dx.doi.org/10.1088/0957-4484/15/1/009

3. Klumpp C, Kostarelos K, Prato M and Bianco A. Functionalized carbon nanotubes as emerging nanovectors for the delivery of therapeutics. *BBA-Biomembranes*. 2006; 1758(3):404-412. PMid:16307724. http://dx.doi.org/10.1016/j.bbamem.2005.10.008

4. Schuch FF, Bevilaqua RCA and Fagan SB. Propriedades eletrônicas e estruturais de nanotubos de carbono e aplicação como carreadores de fármacos. *Disciplinarum Scientia*. 2007; 8(1):95-105.

5. Lobo AO, Corat MAF, Antunes EF, Palma MBS, Pacheco-Soares C, Garcia EE et al. An evaluation of cell proliferation and adhesion on vertically-aligned multi-walled carbon nanotube films. *Carbon*. 2010; 48:245. http://dx.doi.org/10.1016/j.carbon.2009.09.012

6. Lobo AO, Corat MAF, Ramos SC, Matsushima JT, Granato AEC, Pacheco-Soares C et al. Fast Preparation of Hydroxyapatite/Superhydrophilic Vertically Aligned Multiwalled Carbon Nanotube Composites for Bioactive Application. *Langmuir*. 2010; 26:18308-18314. PMid:20961085. http://dx.doi.org/10.1021/la1034646

7. Mendes RM, Silva GAB, Caliari MV, Silva EE, Ladeira LO and Ferreira AJ. Effects of single wall carbon nanotubes and its functionalization with sodium hyaluronate on bone repair. *Life Sciences*. 2010; 87:215-222. PMid:20600151. http://dx.doi.org/10.1016/j.lfs.2010.06.010

8. Thelen S, Barthelat F and Brinson LC. Mechanics considerations for microporous titanium as an orthopedic implant material. *Journal of Biomedical Materials Research*. 2004; 69(4):601-610. PMid:15162401. http://dx.doi.org/10.1002/jbm.a.20100

9. Machado ACP, Oliveira MV, Pereira RP, Carvalho YR and Cairo CAA. In vivo evaluation of porous titanium implants with biomimetic coating. *Key Engineering Materials*. 2009; 396-398:179-182. http://dx.doi.org/10.4028/www.scientific.net/KEM.396-398.179

10. Marsi TCO, Santos TG, Pacheco-Soares C, Corat EJ, Marciano FR and Lobo AO. Biomineralization of Superhydrophilic Vertically Aligned Carbon Nanotubes. *Langmuir*. 2012; 28:4413-4424. PMid:22320358. http://dx.doi.org/10.1021/la300111k

11. Barrere F, Van Blitterswijk CA, De Groot K and Layrolle P. Nucleation of biomimetic Ca–P coatings on Ti6Al4V from a SBF×5 solution: influence of magnesium. *Biomaterials*. 2002; 23(29):2211-2220. http://dx.doi.org/10.1016/S0142-9612(01)00354-4

12. Barrere F, Van Blitterswijk CA, De Groot K and Layrolle P. Influence of ionic strength and carbonate on the Ca-P coating formation from SBF×5 solution. *Biomaterials*. 2002; 23(29):1921-1930. http://dx.doi.org/10.1016/S0142-9612(01)00318-0

13. Kokubo T. Apatite formation on surfaces of ceramics, metals and polymers in body environments. *Acta Biomaterialia*. 1998; 46(7):2519-2527. http://dx.doi.org/10.1016/S1359-6454(98)80036-0

14. Ishizaki T, Saito N and Osamu Takai O. Correlation of Cell Adhesive Behaviors on Superhydrophobic, Superhydrophilic, and Micropatterned Superhydrophobic/Superhydrophilic Surfaces to Their Surface Chemistry. *Langmuir*. 2010; 26, p.8147-8154. PMid:20131757. http://dx.doi.org/10.1021/la904447c

15. Kim Y, Lee D, Oh Y, Choi J and Baik S. The effects of acid treatment methods on the diameter dependent length separation of single walled carbon nanotubes. *Synthetic Metals*. 2006; 156:999-1003. http://dx.doi.org/10.1016/j.synthmet.2006.06.004

16. Lakshminarayanan PV, Toghiani Junior H and Pittman CU. Nitric acid oxidation of vapor grown carbon nanofibers. *Carbon*. 2004; 42:2433-2442. http://dx.doi.org/10.1016/j.carbon.2004.04.040

17. Liu M, Yang Y, Zhu T and Liu Z. Chemical modification of single-walled carbon nanotubes with peroxytrifluoroacetic acid. *Carbon*. 2005; 43:1470-1478. http://dx.doi.org/10.1016/j.carbon.2005.01.023

18. Lobo AO, Marciano FR, Regiani L, Ramos SC, Matsushima JT and Corat EJ. Proposed model for growth preference of plate-like nanohydroxyapatite crystals on superhydrophilic

2013; 16(3)

Proposed Model for Biomineralization of Novel Nanohydroxyapatite/Vertically
Aligned Multiwalled Carbon Nanotube Scaffolds

667

vertically aligned carbon nanotubes by electrodeposition. *Theoretical Chemistry Accounts*. 2011; 130:1071-1082. http://dx.doi.org/10.1007/s00214-011-0993-x

19. Liao S, Xu G, Wang W, Watari F, Cui F, Ramakrishna S et al. Self-assembly of nano-hydroxyapatite on multi-walled carbon nanotubes. *Acta Biomaterialia*. 2007; 3:669-675. PMid:17512807. http://dx.doi.org/10.1016/j.actbio.2007.03.007

20. Kokubo T, Kim HM and Kawashita M. Novel bioactive materials with different mechanical properties. *Biomaterials*. 2003; 24(13):606-8501. http://dx.doi.org/10.1016/S0142-9612(03)00044-9

21. Tung MS. *Calcium Phosphates in Biological and Industrial Systems*. Dordrecht: Kluwer Academic Publishers; 1998.

22. Escada ALA, Machado JPB, Schneider SG, Alves Rezende MCR and Alves Claro APR. Biomimetic calcium phosphate coating on Ti–7.5Mo alloy for dental application. *Journal of Materials Science*: Materials in Medicine. 2011; 22(11):2457-2465. PMid:21909642. http://dx.doi.org/10.1007/s10856-011-4434-0

23. LeGeros RZ. Calcium Phosphates in Oral Biology and Medicine. *Monographs in Oral Science*. 1991; 15:1-201.

24. Dorozhkin SV. Calcium Orthophosphates in Nature, Biology and Medicine. *Materials*. 2009; 2:399-498. http://dx.doi.org/10.3390/ma2020399

25. Chen MF, Yang XJ, Hu RX, Cui ZD and Man HC. Bioactive NiTi shape memory alloy used as bone bonding implants. *Materials Science and Engineering C*. 2004; 4:497-502. http://dx.doi.org/10.1016/j.msec.2003.11.001

**ERRATUM**

In the article: Proposed Model for Biomineralization of Novel Nanohydroxyapatite/Vertically Aligned Multiwalled Carbon Nanotube Scaffolds (http://dx.doi.org/10.1590/S1516-14392013005000039), published ahead of print on March 8th, the correct author's addresses are as follow:

Inacio Regiani
Instituto Tecnológico de Aeronautica – ITA, Praça Marechal Eduardo Gomes, 50, CEP 12228-900, São José dos Campos, SP, Brazil

Anderson Oliveira Lobo
Laboratory of Biomedical Nanotechnology, Universidade do Vale do Paraíba – Univap, Av. Shishima Hifumi, 2911, CEP 12224-000, São José dos Campos, SP, Brazil